Content-color-dependent screening (CCDS) using regular or irregular clustered-dot halftones

Altyngul Jumabayeva
School of Electrical and Computer Engineering
Purdue University
West Lafayette, IN 47907, U.S.A.
ajumabay@purdue.edu

Tal Frank
Hewlett-Packard Indigo Division
Rehovot, Israel
tfrank@hp.com

Yotam Ben-Shoshan
Hewlett-Packard Indigo Division
Rehovot, Israel
yotam.ben-shoshan@hp.com

Robert Ulichney
Hewlett-Packard Laboratories USA
Cambridge, MA 02142, U.S.A.
u@hp.com

Jan Allebach
School of Electrical and Computer Engineering
Purdue University
West Lafayette, IN 47907, U.S.A.
allebach@purdue.edu

***Abstract*—In our previous work, we have presented an HVS-based model for the superposition of two clustered-dot color halftones, which are widely used for electrophotographic printers due to their relatively poor print stability. The model helps us to decide what are the best color assignments for the two regular or irregular halftones that will minimize the perceived error [1]. After applying our model to the superposition of three and four clustered-dot color halftones, it was concluded that this color assignment plays a significant role in image quality. Moreover, for different combinations of colorant absorptance values, their corresponding best color assignments turn out to be different. Hence, in this paper we propose to apply different color assignments within the image depending on the local color and content of the image. If the image content locally has a high variance of color and texture, the artifacts due to halftoning will not be as visible as the artifacts in smooth areas of the image. Therefore, the focus of this paper is to detect smooth areas of the image and apply the best color assigments in those areas. In order to detect smooth areas of the image, it was decided to segment the image based on the color of the content. We used the well-known K-means clustering algorithm along with an edge detection algorithm in order to segment an image into clusters. We then used our spatiochromatic HVS-based model for the superposition of four halftones in order to search for the best color assignment in a particular cluster. This approach is primarily directed towards good quality rendering of large smooth areas, especially areas containing important memory colors, such as flesh tones. We believe that content-color-dependent screening can play an important role for developing high quality printed color images.**

***Index Terms*—Image quality, image segmentation, image edge detection**

I. Introduction

Digital halftoning is the process of rendering a continuous-tone image with a limited number of tone levels. The purpose of digital halftoning is to produce an image with correct tone and detail of the original image without introducing any visible artifacts. There are three most widely used categories of halftoning algorithms: point processes (e.g. screening), neighbourhood processes (e.g. error diffusion), and iterative algorithms [2]. Based on the resulting halftone textures, screens may be classified according to two separate characteristics: 1) dispersed or clustered dots, and 2) periodic or aperiodic. In this paper, we work with the periodic clustered-dot halftones, which are widely used for electrophotographic printers due to their relatively poor print stability.

The purpose of our research is to improve print quality in high end digital presses. One of the main drawbacks of digital presses is their limited capability to approximate the screen frequencies and angles that are conventionally used by traditional offset presses. The combination of screen frequency and angle is conveniently represented by the 2×2 *periodicity matrix* $\mathbf{N} = \left[\mathbf{z}^T \mid \mathbf{w}^T\right]$, where $\mathbf{z} = [z_i, z_j]$ and $\mathbf{w} = [w_i, w_j]$ are two tile vectors with rational entries z_i, z_j, w_i, w_j. The two tile vectors generate a parallelogram, which is also known as the *continuous-parameter halftone cell* (CPHC) with periodicity matrix $\mathbf{N}$. The whole spatial domain can then be tiled by using $n_1\mathbf{z} + n_2\mathbf{w}, (n_1, n_2) \in Z^2$ [1], [3], [4].

One way to achieve a closer approximation to the desired screen frequency and angle is to allow non-integer-valued elements in the periodicity matrix. Such halftones are called *irregular* halftones, since the shapes of the dot clusters may vary from cluster to cluster. On the other hand, if the periodicity matrix has only integer-valued elements, such halftones are called *regular* halftones. In this case, each dot-cluster is identical; but the set of achievable combinations of screen frequency and angle is limited [1] - [5]. In this paper, we will use irregular clustered-dot halftones to demonstrate our results. In order to generate irregular clustered-dot halftones, we followed the method proposed by Baqai and Allebach [6]. Baqai and Allebach presented a systematic method for designing regular clustered-dot halftones based on the periodicity matrix [6]. We extended their approach to design of irregular clustered-dot halftones.

Most color printers use four different colorants, typically

Research supported by the HP Inc., Indigo Division, Rehovot, Israel.

cyan, magenta, yellow, and black (CMYK). In order to produce a color image, each colorant plane is halftoned independently, as if it were a separate monochrome image. Superimposing the four colorant planes halftoned with screens rotated to different angles will give the final image. Superposition of two or more lattices at different angles can produce moire and rosette artifacts. The moire phenomenon refers to a low-frequency structure, which is easily seen at a normal viewing distance. The rosette pattern has circular or polygonal patterns, which is formed as a result of rotating the halftone screens [2]. The conventional screen angles that minimize visible moire and rosette patterns are 75°, 15°, 0°, and 45°for cyan, magenta, yellow, and black, respectively [2], [4]. A slight change in the screen angle or frequency can result in more visible moire and rosette patterns. There are a number of methods for choosing a set of, say four, regular and/or irregular screens that will not result in artifacts when halftone patterns generated with these screens are superimposed [7], [8]. But how to assign a fixed set of screens to individual colorants has been less thoroughly investigated. In our previous work, we presented a method for choosing the best color assignments to two regular or irregular halftones in order to minimize the perceived error. We developed a model based on the human visual system. In order to account for the difference in the responses of the human viewer to luminance and chrominance information, we used the YyCxCz color space. The perceived error helped us to identify the configuration of colors and screens that will improve the appearance of the superposition image [1]. For example, given two irregular halftones with periodicity matrices $\mathbf{N_1} = \begin{bmatrix} 9/2 & -1 \\ 1 & 9/2 \end{bmatrix}$, and $\mathbf{N_2} = \begin{bmatrix} 10/3 & -10/3 \\ 10/3 & 10/3 \end{bmatrix}$, two colorants cyan and magenta with absorptance of 0.25, it was concluded that assigning $\mathbf{N_1}$ to magenta and $\mathbf{N_2}$ to cyan will yield a better result than assigning $\mathbf{N_2}$ to magenta and $\mathbf{N_1}$ to cyan [1].

In the case of 4 periodicity matrices and 4 colorants, we have 24 different ways to assign colors to the periodicity matrices. In addition, if colorants have different absorptance values, then we have to look at all possible combinations of absorptance values. Since any image can contain any color content, i.e. different absorptance values for each colorant, it was decided that the image needed to be clustered. Next, for each cluster in the image, the corresponding best color assignment can be determined and the image can be halftoned with the best color assignments depending on the color content. It turned out that when we switched color assignments inside smooth areas, the transition from one color assignment to another caused an artifact. Hence, an edge detection algorithm was added. Finally, using the cluster-map and the edge-map, we were able to segment the image based on the color content, and halftone each segment with its optimal color assignment, while not segmenting smooth regions with similar color content into separate regions.

The concept of performing image segmentation based on the content and using different halftoning techniques in different regions of the image was investigated before. Park et al developed a method in which they divided a document into smooth and detail objects, and used low-frequency, periodic clustered-dot halftoning in smooth areas to promote stable development, and high-frequency, periodic clustered-dot halftoning in detail areas to provide better rendering of the detail in the image [9]. Ostromoukhov and Nehab checked the local gradient at each pixel, and chose a basic dither matrix based on the magnitude of the gradient [10]. Huang and Bhattacharjya described a process for switching between a periodic, clustered-dot screen in smooth areas, and error diffusion with a screen in detail areas [11]. The screen used for both detail and smooth regions is the same. References [10] and [11] address only halftoning of monochrome images. Reference [9] does consider color. But it is targeted to home/office laser electrophotographic printers, not high-end digital presses. The main novelty of our approach, which is targeted to printing with high-end digital presses, is the application of different color assignments within the image depending on the local color and content of the image, without changing the overall set of screens that are used.

II. Methods

The procedure implemented in our research consists of four parts. In Sec. II-A, the K-means algorithm to cluster the color content is described. In Sec. II-B, an algorithm for obtaining the segmented edge-map is described. In Sec. II-C, merging of the cluster-map and the segmented edge-map into a final map is explained. In Sec. II-D, the approach for obtaining the best color assignment is reviewed and two examples are provided. Finally, the image can be halftoned using the final map of clusters and their corresponding best color assignments. The complete block diagram is presented in Fig. 1.

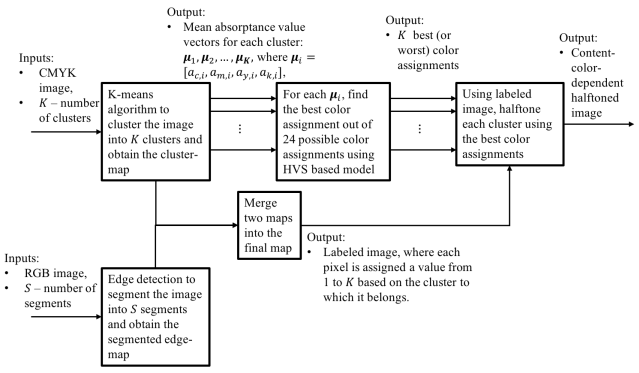

Fig. 1. Block diagram of content-color-dependent screening (CCDS).

A. Generation of the cluster-map using K-means

K-means clustering is a type of unsupervised learning, which can be used when we have unlabeled data that needs to be clustered or categorized into groups based on a certain similarity feature [12]. In our case, we start with a CMYK image, and our goal is to cluster all pixels in the image based on the absorptance values of the C, M, Y and K separations.

The number of clusters is usually represented by the variable K. The algorithm starts with initial estimates for the K centroids. In our approach, the initial centroids were randomly selected from the image. Each centroid represents one of the clusters. Each pixel of the image is then assigned to its nearest centroid's cluster, based on the squared Euclidean distance. Next, by taking the mean of all pixels assigned to that centroid's cluster, the new centroids are obtained. The algorithm iterates until the maximum number of iterations is reached [12]. Based on our experiments, K-means clustering converged before 10 iterations. Therefore, we chose to use the value of 10 as the maximum number of iterations.

The outputs of the K-means clustering algorithm are: a) the final centroids of the K clusters; b) the cluster-map, which is the image indexed with values 1 through K that represent each pixel being assigned to a single cluster. We'll later use the final centroids values in order to obtain the best color assignments out of 24 possible color assignments (i.e. given 4 periodicity matrices, and 4 colorants C, M, Y and K, there are 24 ways to make color assignments). In addition, we will use the cluster-map along with the edge-map in order to build the final map for halftoning the image.

B. Generation of the segmented edge-map

After obtaining the cluster-map and halftoning the image based solely on the cluster map, it was concluded that the transition between two color assignments in smooth areas of the image was very visible. Hence, we need an additional step in which the smooth areas will be identified. In order to do that, it was decided to first generate an edge map of the image, and then use the connected components algorithm to partition the edge image into segments. Since the number of segments may be too large, it was decided that we should only focus on the largest segments and constrain the number of segments to some number S. Therefore, $S-1$ segments will be selected in the order of their decreasing size. The remaining segments will be combined in the last segment. The complete block diagram for obtaining the segmented image is provided in Fig. 2.

As shown in Fig. 2, after converting from RGB to L⋆a⋆b⋆ space, we used a bilateral filter in order to smooth the image while preserving large-scale edges without blurring. The expression for the bilateral filter with the CIE L⋆a⋆b⋆ color difference model is presented in (1) [13], [14].

$$\mathcal{BF}\{I_k[m_0,n_0]\} = \frac{1}{M}\sum_{m=m_0-w}^{m_0+w}\sum_{n=n_0-w}^{n_0+w}\exp\left(-\frac{(m-m_0)^2+(n-n_0)^2}{2\sigma_d^2}\right) \times \exp\left(-\frac{\Delta E^2(I_{L^\star a^\star b^\star}[m,n], I_{L^\star a^\star b^\star}[m_0,n_0])}{2\sigma_r^2}\right) I_k[m,n], \tag{1}$$

where $\mathcal{BF}\{I\}$ is the bilateral filtered image in CIE L⋆a⋆b⋆ color space; $k \in \{L^\star, a^\star, b^\star\}$ refers to one of the channels in the CIE L⋆a⋆b⋆ color space; $[m_0, n_0]$ is the center pixel of a $(2w+1)\times(2w+1)$ convolution window; σ_d is the standard deviation of spatial smoothing; and σ_r indicates the range of tolerance in color difference. We used $\sigma_r = 6$, and for σ_d we used 2% of image diagonal. The color difference component is calculated as the Euclidean distance between the two colors in the CIE L⋆a⋆b⋆ space:

$$\begin{aligned}\Delta E^2(I_{L^\star a^\star b^\star}[m,n], I_{L^\star a^\star b^\star}[m_0,n_0]) &= (I_{L^\star}[m,n] - I_{L^\star}[m_0,n_0])^2 + \\ &(I_{a^\star}[m,n] - I_{a^\star}[m_0,n_0])^2 + \\ &(I_{b^\star}[m,n] - I_{b^\star}[m_0,n_0])^2,\end{aligned} \tag{2}$$

and the normalization factor M is computed as

$$M = \sum_{m=m_0-w}^{m_0+w}\sum_{n=n_0-w}^{n_0+w}\exp\left(-\frac{(m-m_0)^2+(n-n_0)^2}{2\sigma_d^2}\right) \times \exp\left(-\frac{\Delta E^2(I_{L^\star a^\star b^\star}[m,n], I_{L^\star a^\star b^\star}[m_0,n_0])}{2\sigma_r^2}\right). \tag{3}$$

Next, we used a Sobel edge detector in the L⋆a⋆b⋆ space to obtain the magnitude of the gradients in L⋆, a⋆, and b⋆ channels, denoted as $|\nabla g_{L^\star}|$, $|\nabla g_{a^\star}|$ and $|\nabla g_{b^\star}|$ [15], [16]. The magnitude of the color gradient is then computed as

$$|\nabla g_{L^\star a^\star b^\star}| = \sqrt{|\nabla g_{L^\star}|^2 + |\nabla g_{a^\star}|^2 + |\nabla g_{b^\star}|^2}. \tag{4}$$

The initial edge map can then be obtained by applying hysteresis thresholding [17]. In order to thin the edges, we used the well known Zhang-Suen thinning algorithm [18]. After that, the connected components algorithm with a 4-point connectivity was used [19]. Finally, S segments were selected based on the order of decreasing size producing the segmented edge-map.

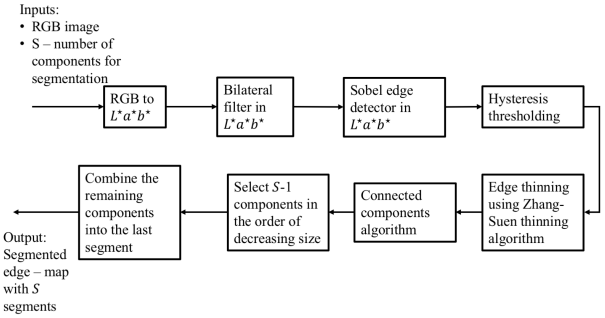

Fig. 2. Block diagram for obtaining segmented edge-map.

C. Merging the cluster-map and the segmented edge-map

After obtaining the cluster-map and the segmented edge-map, the final map needs to be generated. In order to accomplish this goal, the following approach was used. We start with the segmented edge-map, and for each segment $s \in 1, 2, ..., S$, compute the number of pixels that were assigned to each cluster $k \in 1, 2, ..., K$ within this segment. We then determine the cluster number, which occured the maximum number of times among the pixels in that segment. Finally, we assign that number to all the pixels in the segment.

As a result, we obtained the final map with K clusters that would be used for halftoning the image with different color assignments.

D. Selection of the best color assignments

In order to select the best color assignment for any set of absorptance values $a_{cmyk} = (a_c, a_m, a_y, a_k)$, the HVS-based model for the superposition of color halftones was used [1]. In our case, we've narrowed down all image absorptance values to the mean absorptance values of the K clusters obtained in Sec. II-A, specified as $\mu_1, ..., \mu_k$, where each $\mu_i = (a_{c,i}, a_{m,i}, a_{y,i}, a_{k,i})$. Hence, for each of the K vectors of mean absorptance values, the best color assignment was obtained. The metric for obtaining the best color assignment was presented in [1] , and is denoted as $\Delta E_{fluctuation}$ (previously $\Delta E_{average}$) .

Next, two examples comparing different color assignments are presented. For both examples, the following geometries were used:

$$\mathbf{N_1} = \begin{bmatrix} 4.56 & -1.19 \\ 1.19 & 4.56 \end{bmatrix}, \mathbf{N_2} = \begin{bmatrix} 3.44 & -3.26 \\ 3.26 & 3.44 \end{bmatrix} \quad (5)$$
$$\mathbf{N_3} = \begin{bmatrix} 1.30 & -4.45 \\ 4.45 & 1.30 \end{bmatrix}, \mathbf{N_4} = \begin{bmatrix} 2.50 & -2.40 \\ 2.40 & 2.50 \end{bmatrix}.$$

For the HP Indigo press with resolution 812.8 dpi, the parameters for the 4 geometries above are: 172.5 lpi and 14.62°, 171.56 lpi and 43.45°, 175.17 lpi and 73.74°, and 234.73 lpi and 43.83°. In order to represent the color assignment, a 4-digit number is used. Each digit in a color assignment number represents the periodicity matrix number being assigned to C, M, Y, and K. For example, color assignment number 3214 should be interpreted as $\mathbf{N_3}$ is cyan, $\mathbf{N_2}$ is magenta, $\mathbf{N_1}$ is yellow, and $\mathbf{N_4}$ is black.

For Example 1 in Fig. 3, the set of absorptance values is $a_{cmyk} = (0.20, 0.93, 0.96, 0.13)$ with the color assignments 3421 and 3214, and the resulting $\Delta E_{fluctuation}$ values are 0.92 and 3.89, accordingly. It can be seen that the superposition image with color assignment 3421 is much smoother than the superposition image with color assignment 3214, and hence its $\Delta E_{fluctuation}$ is smaller. Similarly, a second example is demonstrated with superposition images in Fig. 4. The set of absorptance values for these images is $a_{cmyk} = (0.29, 0.31, 0.30, 0.02)$, and the color assignments are 3412 and 4231. The resulting $\Delta E_{fluctuation}$ values are 4.78 and 6.91, respectively.

III. EXPERIMENTAL RESULTS

In order to demonstrate a result of CCDS, it was decided to use the image shown in Fig. 5 (a). The K-means clustering algorithm was applied with the number of clusters $K = 4$. The cluster-map can be observed in Fig. 5 (b). Based on the cluster-map, it was concluded that since smooth areas of the image, such as the woman's face and arms, got clustered into two clusters, the additional edge-detection and segmentation step was important. Otherwise, we will see artifacts from the transition between two color assignments after halftoning. The

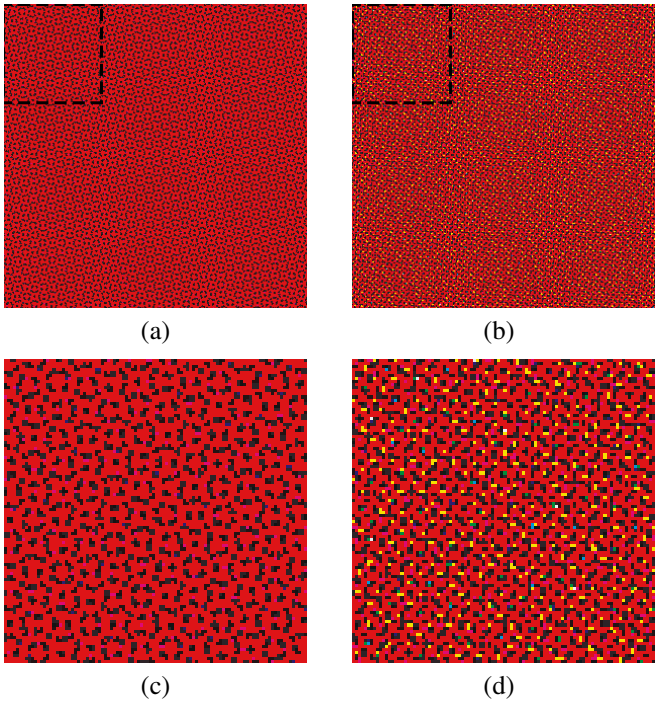

Fig. 3. Example 1: $a_{cmyk} = (0.20, 0.93, 0.96, 0.13)$ (a) color assignment 3421, $\Delta E_{fluctuation} = 0.92$; (b) color assignment 3214, $\Delta E_{fluctuation} = 3.89$; (c) zoomed-in part of the image outlined in (a); (d) zoomed-in part of the image outlined in (b)

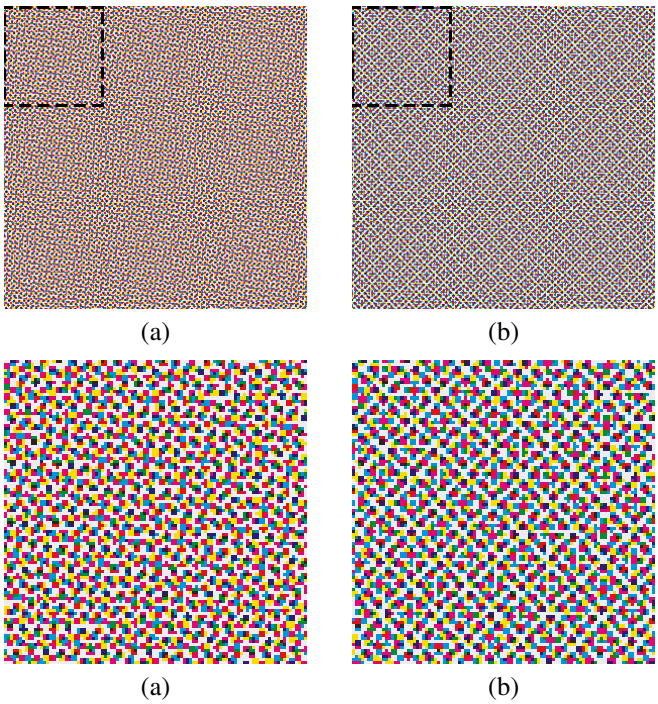

Fig. 4. Example 2: $a_{cmyk} = (0.29, 0.31, 0.30, 0.02)$ (a) color assignment 3412, $\Delta E_{fluctuation} = 4.78$; (b) color assignment 4231, $\Delta E_{fluctuation} = 6.91$; (c) zoomed-in part of the image outlined in (a); (d) zoomed-in part of the image outlined in (b)

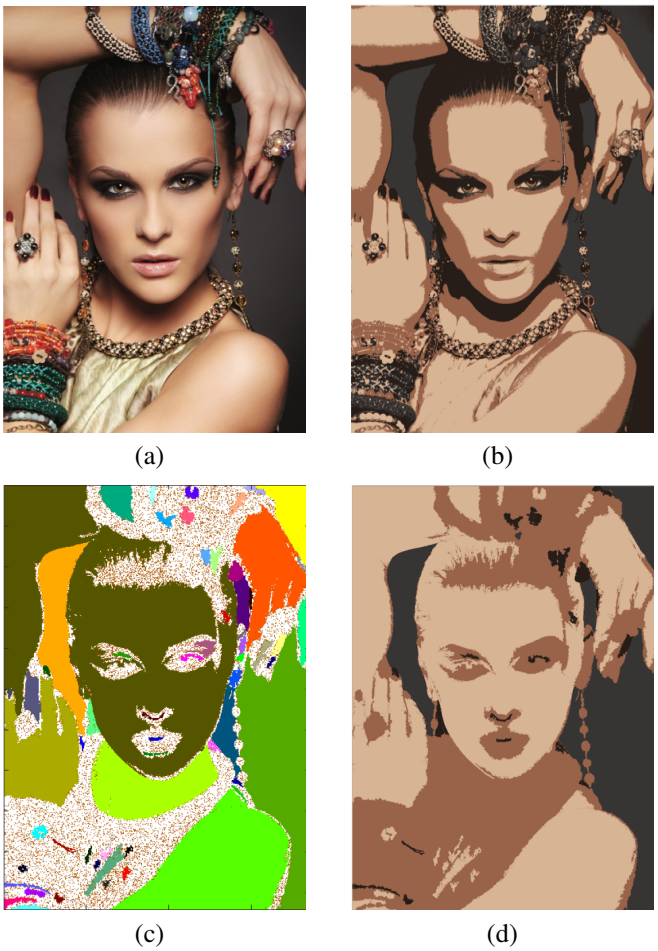

Fig. 5. Example of obtaining the map for selecting best color assignments in a given image: (a) Original image; (b) Cluster-map; (c) Segmented edge-map; d) Final map: merging of cluster-map and segmented edge-map.

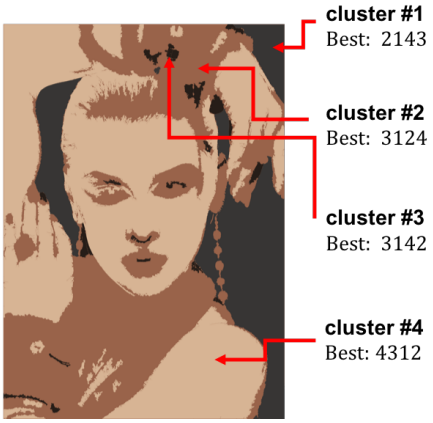

Fig. 6. Best color assignments for the four clusters comprising the image.

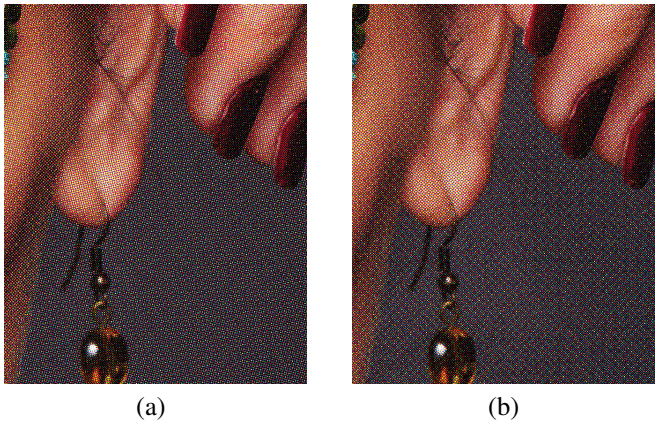

Fig. 7. (a) Halftoning with CCDS applied: optimal color assignments were used for the clusters shown in Fig. 6; (b) Halftoning with the single color assignment 3214 for the entire image. (The reader is advised to zoom into to 300% magnification in order to obtain a more accurate impression of these two halftone images.)

result of the segmented edge-map with $S = 4$ is presented in Fig. 5 (c). After that, the final map, which involves merging the maps in Fig. 5 (b) and (c), was obtained and is displayed in Fig. 5 (d). It can be seen that each smooth area of the image is assigned a single cluster. Hence, after halftoning, the visible artifacts in those areas will no longer be present. After that, we used our HVS-based model to determine the color assignments that will minimize the perceived error for the four clusters [1]. The best color assignments with their corresponding clusters are presented in Fig. 6. Finally, using the geometries presented in Sec. II-D, a part of the halftoned image is presented in Fig. 7 (a). The image in Fig. 7 (b) is generated by halftoning using the single color assignment of 3214 for the entire image. The assignment of 3214 was chosen randomly out of 24 possible color assignments. By comparing the images in Figs. 7 (a) and (b), it can be concluded that the image in Fig. 7 (a) is much smoother than the image in Fig. 7 (b). Therefore, applying content-color-dependent screening yields much smoother images than the images obtained by using a single color assignment for the entire image.

IV. CONCLUSION

We have presented a content-color-dependent screening method using clustered-dot color halftones, which helps us produce prints with better quality. We used the K-means algorithm along with edge detection to segment an image depending on its color content. Then, we used an HVS-based model to select the best color assignment for each of the clusters in the image. Since the HVS-based model determines the color assignments that will minimize the perceived error, and the entire image will be halftoned with the best color assignments based on the color content, we believe that the CCDS approach can move the quality of color prints generated by limited-resolution digital presses closer to that of the much higher resolution analog offset printing presses with which the digital presses are competing.

REFERENCES

[1] A. Jumabayeva, T. Frank, Y. Ben-Shoshan, R. Ulichney, and J. Allebach, "HVS-based model for superposition of two color halftones," in *Color Imaging XXI: Displaying, Processing, Hardcopy, and Applications*, vol. 2016, Part of IS&T Electronic Imaging 2016, San Francisco, CA, Feb. 2016.

[2] H. Kang, *Digital Color Halftoning*. Bellingham, WA: SPIE The International Society for Optical Engineering, 1999.

[3] A. Jumabayeva, Y.-T. Chen, T. Frank, R. Ulichney, and J. Allebach, "Design of irregular screen sets that generate maximally smooth halftone patterns," in *Color Imaging XX: Displaying, Processing, Hardcopy, and Applications*, vol. 9395, Part of SPIE/IS&T Electronic Imaging, San Francisco, CA, Feb. 2015.

[4] Y. Chen, T. Kashti, M. Fischer, D. Shaked, R. Ulichney, and J. P. Allebach, "The lattice-based screen set: a square n - color all-orders moiré-free screen set," in *IEEE Transactions on Image Processing*, vol. 25, Apr. 2016, pp. 1873 – 1886.

[5] A. Jumabayeva, Y.-T. Chen, T. Frank, R. Ulichney, and J. Allebach, "Single separation analysis for clustered dot halftones," in *Proceedings of the 2016 IEEE International Conference on Image Processing*, Phoenix, AZ, Sep. 2016, pp. 4383 – 4387.

[6] F. A. Baqai and J. P. Allebach, "Computer-aided design of clustered-dot color screens based on a human visual system model," in *Proceeding of the IEEE*, vol. 90, Jan. 2002, pp. 104–122.

[7] J.-Y. Kim, Y.-Y. Chen, M. Fischer, O. Shacham, C. Staelin, and J. P. Allebach, "Design of color screen sets for robustness to color plane misregistration," in *Proceedings of the 2011 IEEE International Conference on Image Processing*, Brussels, Belgium, Sep. 2011, pp. 1733–1736.

[8] J.-Y. Kim, Y.-Y. Chen, M. Fischer, O. Shacham, C. Staelin, K. Bengston, and J. P. Allebach, "Design of screen tile vectors," in *Color Imaging XVI: Displaying, Processing, Hardcopy, and Applications*, vol. 7866, Part of SPIE/IS&T Electronic Imaging, San Francisco, CA, Jan. 2011.

[9] S. J. Park, M. Q. Shaw, G. Kerby, T. Nelson, D.-Y. Tzeng, K. R. Bengston, and J. P. Allebach, "Halftone blending between smooth and detail screens to improve print quality with electrophotographic printers," in *IEEE Transactions on Image Processing*, vol. 25, Feb. 2016, pp. 601 – 614.

[10] V. Ostromoukhov and S. Nehab, "Halftoning with gradient-based selection of dither matrices," U.S. Patent 5 701 366, Dec. 1997.

[11] J. Huang and A. Bhattacharjya, "An adaptive halftone algorithm for composite documents," in *Color Imaging IX: Processing, Hardcopy, and Applications*, vol. 5293, Part of SPIE/IS&T Electronic Imaging, San Jose, CA, Dec. 2003.

[12] J. MacQueen, "Some methods for classification and analysis of multivariate observations," in *Proceedings of the Fifth Berkeley Symposium on Mathematical Statistics and Probability*, vol. 1, University of California Press, Oakland, CA, 1967, pp. 281–297.

[13] K. McLaren, "The development of the CIE 1976 (L*a*b*) uniform colour space and colour-difference formula," in *Journal of the Society of Dyers and Colourists*, vol. 92, no. 9, Blackwell Publishing Ltd, 1976, pp. 338–341.

[14] S. Hu, Z. Pizlo, and J. P. Allebach, "JPEG ringing artifact visibility evaluation," in *Image Quality and System Performance XI*, vol. 9016, Part of SPIE/IS&T Electronic Imaging, San Francisco, CA, Feb. 2014.

[15] P.-E. Danielsson and O. Seger, "Generalized and separable sobel operators," in *Machine Vision for Three-Dimensional Scenes*, H. Freeman, Ed. Orlando, FL: Academic Press, Inc., Jul. 1990, pp. 347 – 381.

[16] X. Feng and J. P. Allebach, "Measurement of ringing artifacts in JPEG images," in *Digital Publishing*, vol. 6076, Part of SPIE/IS&T Electronic Imaging, San Jose, CA, Feb. 2006.

[17] J. Canny, "A computational approach to edge detection," in *IEEE Transactions on Pattern Analysis and Machine Intelligence*, vol. 8, Nov. 1986, pp. 679–698.

[18] T. Zhang and C. Y. Suen, "A fast parallel algorithm for thinning digital patterns," in *Communications of the ACM*, vol. 27, Mar. 1984, pp. 236–239.

[19] L. G. Shapiro and R. M. Haralick, *Computer and Robot Vision*. Boston, MA: Addison-Wesley Longman Publishing Co., Inc., 1992, vol. 1.